Journal of Fibers and Polymer Composites 1 (1): 66-72 (2022)

Journal of Fibers and Polymer Composites

https://journals.gesociety.org/index.php/jfpc/index

EFFECT OF SODIUM IN LiNi$_{0,5}$Mn$_{0,3}$Co$_{0,2}$O$_2$ AS A LITHIUM ION BATTERY CATHODE MATERIAL BY SOLID STATE REACTION METHOD

Yustinus Purwamargapratala[1*], Indra Gunawan[2], D.N.Haerani[2], Sudirman[2]
Evvy Kartini[2], Anne Zulfia[1], Alexey Glushenkov[7]

[1]Department of Metalurgy and Material Engineering, University of Indonesia
[2] National Research and Innovation Agency
[7]Australian National University, Canberra.

*Corresponding author
pratala_yustinus@yahoo.com

Abstract. *Lithium-ion batteries (LIBs) have become widely used powder sources for portable electronics and electric vehicles. The discovery of lithium nickel manganese cobalt oxide ($LiNi_{0.5}Mn_{0.3}Co_{0.2}O_2$, NMC532), tremendous efforts have been paid to the development of Ni-rich layer-structured NMC532 materials due to its high capacity when charged to potentials higher than 4.3 V vs Li^+/Li. In this work we report effect of Sodidium in NMC532 layer, the characterization was done by using X-Ray Diffractometer (XRD) to investigate the crystal structure, Electrochemical impedance spectroscopy (EIS) was used to illustrate the resistance change during cycling. The particles morphology and surface chemistry characterizations of both cathode and anode electrodes were performed on Scanning Electron Microscope (SEM). The XRD pattern of the sample shows diffraction peaks at $2\theta = 18.663\,^o$, $36.773\,^o$, $44.459\,^o$, $48.611\,^o$, $58.604\,^o$, $64.322\,^o$, $65.069\,^o$, $68.339\,^o$ and $77.798\,^o$. Na does not affect the NMC532 lattice parameters, which means that Na which is expected to substitute for Li does not occur. The NMC532 conductivity with the addition of Na=0.03 showed a slightly lower value than the NMC532 conductivity with the addition of Na=0.01. Meanwhile, the highest conductivity was seen at NMC532 with the addition of Na=0.05. The addition of Na to NMC532 did not increase the conductivity linearly. SEM images of NMC532 and NMC532 with the addition of Na=0.01; Na = 0.03 and Na = 0.05 can be seen that the Na flakes wrap around the NMC532 granules. The Na flakes surrounding the NMC532 grains at Na = 0.01 were more abundant than the Na flakes surrounding the NMC532 at Na = 0.03.*

***Keywords**: NMC532; Na addition; characterization.*

1. Introduction

Lithium-ion batteries (LIBs) have become widely used power sources for portable electronics and electric vehicles [1-4]. To massively commercialize electric vehicles, the development of Li-ion batteries with higher energy and power density is essential. To this end, extensive research on exploring new cathode materials with an elevated operating voltage (>4.5 V vs Li/Li+) and specific capacity has been carried out. Because of the discovery of lithium

Received March 18, 2022; Accepted March 24, 2022; Published March 30, 2022
https://doi.org//10.55043/jfpc.v1i1.41

nickel manganese cobalt oxide ($LiNi_{0.5}Mn_{0.3}Co_{0.2}O_2$, NMC532), tremendous efforts have been paid to the development of Ni-rich layer-structured NMC materials due to its high capacity when charged to potentials higher than 4.3 V vs Li^+/Li [5].

Overall, the chemistries LIBs are constantly evolving, and in terms of cathode materials, $LiNi_xMn_yCo_{1-x-y}O_2$ (NMC) layered oxides have received increasing attention due to their enhanced specific capacity and thermal stability. As compared with $LiMO_2$ (M = Ni, Mn, or Co) cathodes, NMC-based cathodes also possess the combined merits of three transition metals in which nickel can offer high specific capacities, whereas Co and Mn can provide layered structures and enhanced structural integrity. In addition, NMC-based cathodes can outperform lithium iron phosphate (LFP) cathodes in many areas, particularly in terms of operating voltage in which LFP-based LIBs can only output voltages below 3.4 V and suffer from high rates of self-discharge. Moreover, materials such as Li_2MnO_3 and lithium titanate do not possess great indus- trial potential as cathodes due to short lifespans and high costs [6-8].

Novel high capacity cathode materials (4250 $mAh.g_{-1}$), such as Li_2FeSiO_4 and $Li_2FePO_4F_4$ (yielding 323 and 292 $mAh.g^{-1}$, respectively), have been explored [9]. Another strategy is to increase the operating voltage over 5 V (vs. Li+/Li, hereafter all potentials are given vs. Li^+/Li). Cathode materials of this kind have been developed, too, including olivine-type LiNiPO4 and $LiCoPO_4$ and spinel-type $LiNi_{0.5}Mn_{1.5}O_4$ (LNMO) and $LiCoMnO_4$ [10][11]. The state-of-the-art $LiNi_xMn_yCo_zO_2$ (NMC) cathode is usually charged to 4.2 V or 4.3 V, which only utilizes part of its capacity (287 $mAh.g^{-1}$). Further increase in the charging voltage is also effective in enhancing its capacity and energy. However, to take full advantage of these high-voltage, high-energy cathodematerials, novel electrolytes with high oxidation stability would be required [12]. For example, Li_2CoPO_4F was initially proposed as a high-capacity, high-voltage cathode, but in reality, this material showed a disappointingly low specific capacity of 120 $mAh.g^{-1}$ and a low energy density comparable to $LiCoPO_4$; this poor performance was traced to electrolyte degradation on the energized cathode surface. Another example, the Ni-rich NMC532, is capable of still greater capacity when operated at potentials 44.5 V. However, the battery performance fades rapidly at such potentials due to the parasitic reaction of the conventional carbonate electrolytes on the charged cathode surface and instability in the cathode material itself, causing transition metal ion dissolution into the electrolyte solution [1][13].

In this work we report effect of Sodidium in NMC532 layer, the characterizations was done by using X-Ray Diffractometer (XRD) to investigate the crystal structure, Electrochemical impedance spectroscopy (EIS) was used to illustrate the resistance change during cycling. The particles morphology and surface chemistry characterizations of both cathode and anode electrodes were performed on Scanning Electron Microscope (SEM).

2. Methods

$LiNi_{0.5}Mn_{0.3}Co_{0.2}O_2$ (NMC532) powder was mixed with sodium chloride powder so that the Na content was 0.0%, 1%, 3%, and 5%. Then stirred with a planetary ball mill for 8 hours and sintered in a furnace at 800 °C for 4 hours. The sintered powder was characterized using X-Ray Difraction (XRD, Shimadzu XD 610, Japan. Scanning Electron Microscope (SEM, JEOL JSM 6510 LA, Japan and conductivity measurement by using LCR meter (HIOKI 3532-50, China(. The X-ray diffraction (XRD) measurement was carried out using a Cu Kα radiation source (λ=1.5406 Å), with a step size of 4° min^{-1} from 10 to 80°.

3. Result And Discussion

The effect of Na namely Na = 0.01; 0.03 and 0.05 to the NMC532 structures studied by XRD are shown in Figure 1. The XRD pattern of the sample shows diffraction peaks at 2θ = 18.663 °, 36.773 °, 44.459 °, 48.611 °, 58.604 °, 64.322 °, 65.069 °, 68.339 ° and 77.798 °. The effect of Na on the NMC532 lattice parameters is shown in Table 1.

Table 1. The effect of Na on the NMC532 lattice parameters.

Amount of Na	Lattice parameter (Å)		
	a	b	c
0.01	2.865	2.865	14.252
0.03	2.865	2.865	14.252
0.05	2.865	2.865	14.252

From Table 1 above, Na does not affect the NMC532 lattice parameters, which means that Na which is expected to substitute for Li does not occur.

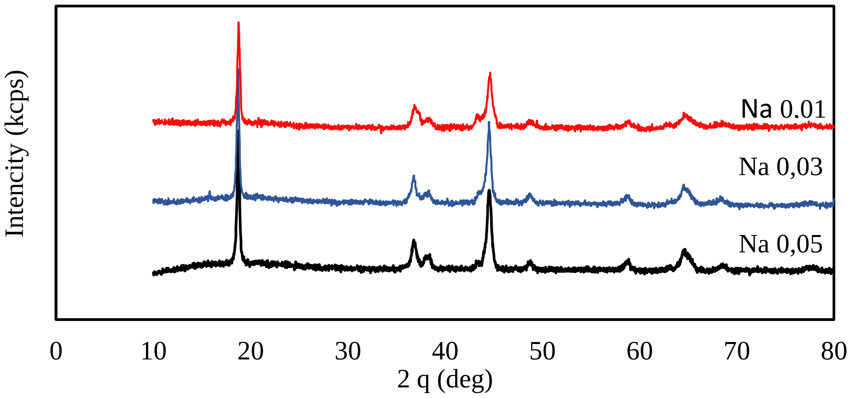

Fig. 1 The effect of Na on the NMC532 structures studied by XRD

The electrical conductivity of the electrolyte was calculated by equation, $\sigma = \lambda/(RbXA)$ where Rb is the bulk resistance from AC impedance, λ the film thickness and A the surface area of electrode. The conductivity of the material as a whole is a function of frequency, the graph in Fig. 2 shows the electrical conductivity of NMC532 has the shape of straight lines at frequencies up to 800 kHz, and then increased with increasing frequency. At low frequencies up to 800 kHz the electrical conductivity is measured following the phenomenon of DC conductivity, and then increased with the increasing frequency following the phenomenon of AC conductivity. DC conductivity is frequency independent conductivity typically assigned to the hopping conduction and AC conductivity has a power-law behavior in terms of frequency. There are tree effects that contribute to the AC conductivity: (i) electrode effects (active at low frequencies), (ii) DC plateau (at intermediate frequencies) and (iii) defect process [14]. The conductivity of MNC measured by LCR is, C = 1,8 268 x 10^{-5} S.cm^{-1}.

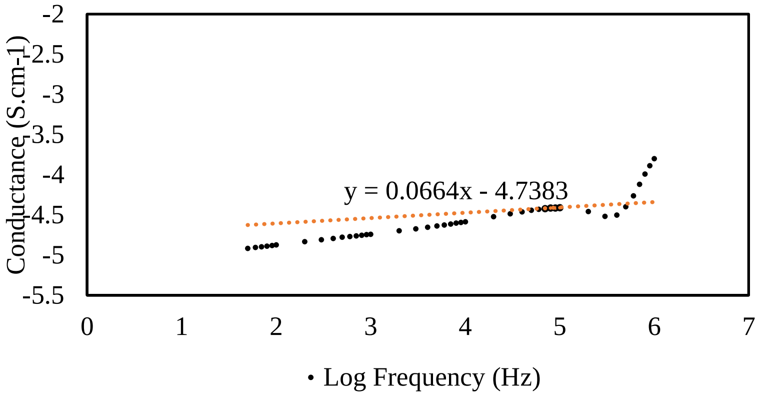

Fig. 2 The graph of electrical conductivity of NMC532.

Fig. 3 shows the plot of conductivity vs log frequency from the sample namely 0.01 Na, 0.03 Na and 0.05 Na. The NMC532 conductivity with the addition of Na=0.03 showed a slightly lower value than the NMC532 conductivity with the addition of Na=0.01. Meanwhile, the highest conductivity was seen at NMC532 with the addition of Na=0.05. The addition of Na to NMC532 did not increase the conductivity linearly.

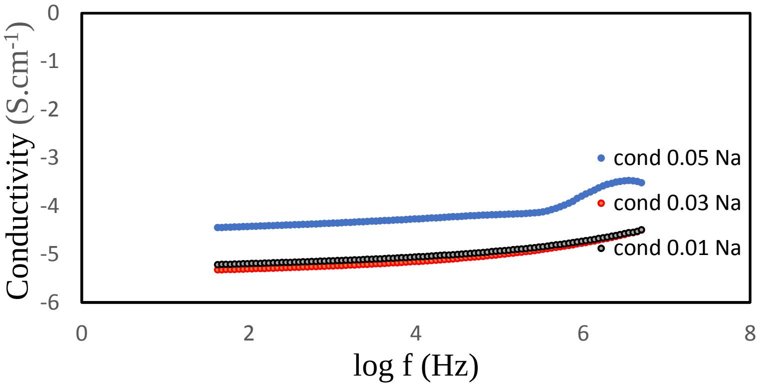

Fig. 3 Plot of conductivity vs log frequency from the sample namely 0.01 Na, 0.03 Na and 0.05 Na.

SEM images of NMC532 and NMC532 with the addition of Na=0.01; Na = 0.03 and Na = 0.05 can be seen in Figure 4. From Figure 4 it is clear that the Na flakes wrap around the NMC532 granules. The Na flakes surrounding the NMC532 grains at Na = 0.01 were more abundant than the Na flakes surrounding the NMC532 at Na = 0.03. This causes the NMC532 conductivity at Na=0.01 to be higher than the NMC532 conductivity at Na=0.03. It is not clear why the addition of Na = 0.03 distribution is less than Na = 0.01 flakes in NMC532. The NMC532 granules themselves as shown in Figure 4a show an agglomeration of NMC532 particles with a size of about 15 microns. These agglomerated particles are composed of small NMC532 particles with a size of less than 1 micron.

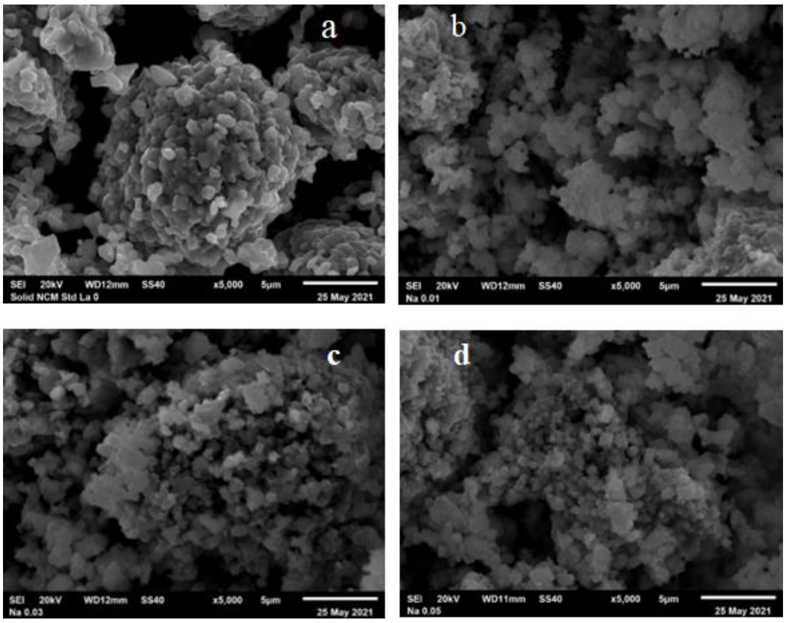

Figure 4. SEM images of NMC532 and NMC532 with the addition of a. Na = 0,0; b. Na=0.01; c. Na = 0.03 and d. Na = 0.05.

Conclusion

The XRD pattern of the sample shows diffraction peaks at $2\theta = 18.663^{o}$, 36.773^{o}, 44.459^{o}, 48.611^{o}, 58.604^{o}, 64.322^{o}, 65.069^{o}, 68.339^{o} and 77.798^{o}. Na does not affect the NMC532 lattice parameters, which means that Na which is expected to substitute for Li does not occur. The NMC532 conductivity with the addition of Na=0.03 showed a slightly lower value than the NMC532 conductivity with the addition of Na=0.01. Meanwhile, the highest conductivity was seen at NMC532 with the addition of Na=0.05. The addition of Na to NMC532 did not increase the conductivity linearly. SEM images of NMC532 and NMC532 with the addition of Na=0.01; Na = 0.03 and Na = 0.05 can be seen that the Na flakes wrap around the NMC532 granules. The Na flakes surrounding the NMC532 grains at Na = 0.01 were more abundant than the Na flakes surrounding the NMC532 at Na = 0.03.

Acknowledgement

There is no conflict of interest in the writing of this paper. We greatly appreciate the financial support from the Ministry of Research, Technology and Higher Education of the Republic of Indonesia, Australian National University, and our gratitude goes to the Advanced Materials Research Center, BRIN, and the Department of Metallurgical and Materials Engineering, the University of Indonesia for their support.

REFERENCES

[1] C. Su, M. He, P. C. Redfern, L. A. Curtiss, I. A. Shkrob, and Z. Zhang, “Environmental Science for high voltage high energy lithium-ion batteries,” *Energy Environ. Sci.*, vol. 10, pp. 900–904, 2017.

[2] E. R. Logan and J. R. Dahn, “Electrolyte Design for Fast-Charging Li-Ion Batteries,” *Trends Chem.*, pp. 1–13, 2020.

[3] C. Wang *et al.*, “Nano Energy Unveiling the critical role of interfacial ionic conductivity in all-solid-state lithium batteries,” *Nano Energy*, vol. 72, no. February, p. 104686, 2020.

[4] C. Wang *et al.*, “Single crystal cathodes enabling high-performance all-solid-state lithium-ion batteries,” *Energy Storage Mater.*, vol. 30, no. March, pp. 98–103, 2020.

[5] C. Su *et al.*, “Functionality Selection Principle for High Voltage Lithium-ion Battery Electrolyte Additives,” 2017.

[6] T. Li, X. Zi, Y. Lei, Z. Datong, S. Kaiyuan, and S. Christina, "Degradation Mechanisms and Mitigation Strategies of Nickel ‐ Rich NMC ‐ Based Lithium" ‐ *Ion Batteries*,

vol. 3, no. 1. Springer Singapore, 2020.

[7] Purwamargapratala, Y., Sudaryanto, & Akbar, dan F. "Neutron tomography study of a lithium-ion coin battery". *Journal of Physics: Conference Series, 1436, 012029.* doi: https://doi.org/10.1088/1742-6596/1436/1/012029, 2020.

[8] S. P. Ong, A. Jain, G. Hautier, B. Kang, and G. Ceder, "Thermal stabilities of delithiated olivine MPO4 (M = Fe, Mn) cathodes investigated using first principles calculations," *Electrochem. commun.*, vol. 12, no. 3, pp. 427–430, 2010.

[9] J. W. Zhao, S. X. Zhao, X. Wu, H. M. Cheng, and C. W. Nan, "Double role of silicon in improving the rate performance of LiFePO4 cathode materials," *J. Alloys Compd.*, vol. 699, pp. 849–855, 2017.

[10] Frank, Jason, "Challenges and Opportunities of Layered Cathodes of LiNixMnyCo (1-x-y) O2 for High-Performance Lithium-ion Batteries". Mechanical Engineering Undergraduate Honors Theses. 81. https://scholarworks.uark.edu/meeguht/81, 2019

[11] Purwamargapratala, Yustinus; Sujatno, Agus; Sabayu, Yohanes Lugas; Kartini, Evvy. "Synthesis of $Li_4Ti_5O_{12}$ (LTO) by Sol-Gel Method for Lithium Ion Battery Anode." *IOP Conference Series: Materials Science and Engineering, 553(2019), 012062–*. doi: https://doi.org/10.1088/1757-899X/553/1/012062, 2019.

[12] L. I. Ling-jun, L. I. Xin-hai, and W. Zhi-xing, "Synthesis of LiNi0.8Co0.1Mn0.1O2 cathode material by chloride co-precipitation method," *Trans. Nonferrous Met. Soc. China*, vol. 20, pp. 279–282, 2010.

[13] L.Zhang, J.Jiang, and W. Zhang, "Capacity Decay Mechanism of the LCO+ NMC532/ Graphite Cells Combined with Post-Mortem Technique," *Energy*, vol. 10, no. 1147, 2017.

[14] I. Gunawan, Deswita, B. Sugeng, and Sudaryanto, "Synthesis and characterization of PVA blended $LiClO_4$ as electrolyte material for battery Li-ion," *IOP Conf. Ser. Mater. Sci. Eng.*, 2017.